Physics Letters A 372 (2008) 6193–6196

Contents lists available at ScienceDirect

Physics Letters A

www.elsevier.com/locate/pla

Measurement-induced decoherence in electronic interferometry at nanoscale

V. Moldoveanu [a], B. Tanatar [b,*], M. Ţolea [a]

[a] National Institute of Materials Physics, PO Box MG-7, Bucharest-Magurele, Romania
[b] Department of Physics, Bilkent University, Bilkent, 06800 Ankara, Turkey

ARTICLE INFO

Article history:
Received 21 July 2008
Accepted 28 July 2008
Available online 30 August 2008
Communicated by V.M. Agranovich

PACS:
73.23.Hk
85.35.Ds
85.35.Be
73.21.La

Keywords:
Quantum interference
Controlled dephasing
Aharonov–Bohm interferometers

ABSTRACT

We introduce a theoretical formalism describing a wide class of 'Which Path' experiments in mesoscopic/nanoscopic transport. The physical system involves a mesoscopic interferometer (e.g. an Aharonov–Bohm ring with embedded dots or a side-coupled quantum dot) which is electrostatically coupled to a nearby quantum point constriction. Due to the charge sensing effect the latter acts as a charge detector. Therefore the interference pattern can be monitored indirectly by looking at the current characteristics of the detector as shown in the experimental work of Buks et al. [E. Buks, R. Schuster, M. Heiblum, D. Mahalu, V. Umansky, Nature (London) 391 (1998) 871]. We use the non-equilibrium Green–Keldysh formalism and a second order perturbative treatment of the Coulomb interaction in order to compute the relevant transport properties. It is shown that in the presence of the Coulomb interaction the current through the detector exhibits oscillations as a function of the magnetic field applied on a single-dot AB interferometer. We also discuss the dependence of the visibility of the Aharonov–Bohm oscillations on the gate potential applied to the dot.

1. Introduction

The quantum interference is one of the hallmarks of mesoscopic physics and it is hard to overestimate its role in the context of present and forthcoming nanoelectronics. Due to the greatly improved semiconductor growth techniques it was possible to provide clear illustrations of quantum coherence in electronic transport at nanoscale. Typical examples are the Aharonov–Bohm oscillations of the current in nanorings with embedded dots [1–3] or the mesoscopic Fano effect. [4] In particular, the transport experiments using interferometers with quantum dots mentioned above showed that the electron–electron interaction, which is certainly inherent in such highly confined systems, does not destroy entirely the quantum coherence. This fact opened the possibility of using detection schemes, namely clever geometries in which a mesoscopic system is coupled only via the Coulomb interaction to a nearby system. The principle of the detection schemes relies heavily on the charge sensing effect: in spite of the fact that there is no charge transfer between the two subsystems the Coulomb interaction implies that any change in the occupation number of the interferometer is felt by the detector and vice versa. Nowadays the charge sensing effect is commonly used in experiments.

When the sensing effect is used in mesoscopic interferometry one has to face a built-in phenomenon, the so-called dephasing. Originally, this concept was introduced in order to describe the reduction of quantum coherence due to inelastic processes induced by the coupling to a phonon bath or by electron–electron interaction [5]. Obviously, the coupling to a phonon bath or the electron–electron interactions in a quantum dot are not easily controlled in actual experiments. Nevertheless, for two Coulomb coupled subsystems, as is the case with interferometer–detector geometry, one can tune various parameters: the bias applied on the detector, the distance between the detector and the relevant region of the interferometer which is detected etc. Therefore, if the Coulomb interaction leads to decoherence during the measurement operation this effect can be controlled.

In this Letter we first review the theoretical description of the charge sensing effect and controlled dephasing within the non-equilibrium Green–Keldysh formalism. The interferometer we consider was realized experimentally by Buks et al. [6] and contains a mesoscopic ring with an embedded dot and a nearby quantum point constriction (QPC) which plays the role of the detector. This experiment was the first clear observation of the controlled dephasing. More precisely, it is found that the visibility of the Aharonov–Bohm oscillations is reduced when a finite bias is applied to the detector. In turn, for a very small bias no clear dephasing was observed. From the physical point of view, applying the bias on the quantum point constriction increases the number

* Corresponding author.
E-mail address: tanatar@fen.bilkent.edu.tr (B. Tanatar).

0375-9601/$ – see front matter
doi:10.1016/j.physleta.2008.07.079

of electrons that pass through it, increasing therefore the sensitivity of the detector.

Various methods were used to approach the controlled dephasing problem from the theoretical point of view. Aleiner et al. [7] used quantum field theoretical methods to compute the dephasing rate. Levinson [8] studied the dephasing of a single level QD coupled to a detector within the influence functional approach. Hackenbroich [9] performed a master equation calculation of the off-diagonal elements of the statistical operator of the same system. Finally, Silva and Levit [10] discussed the dephasing for a single level QD coupled to a quantum point constriction within the Keldysh formalism.

The aim of this Letter is to complement the results presented in Ref. [11] for a single-dot Aharonov–Bohm interferometer Coulomb coupled to a charge detector, by considering in more detail the effects of the location of the bias window with respect to the spectrum of the truncated ring that gives the background signal in the Fano line and of the magnetic flux. We also pay particular attention to the visibility of the Aharonov–Bohm oscillations and show its behavior as a function of the gate potential applied on the embedded quantum dot. The Letter is organized as follows. Section 2 gives the relevant formal details and Section 3 presents numerical results. We conclude with a brief summary in Section 4.

2. Theory

We describe our systems by tight binding Hamiltonians. The general form is the following:

$$H(t) = H_{\mathrm{I}} + H_{\mathrm{L}} + H_{\mathrm{D}} + \chi_\eta(t)(H_i + H_t), \tag{1}$$

where H_{I}, H_{D}, H_{L} stand for the Hamiltonian of the disconnected noninteracting subsystems (interferometer (I), detector (D), leads (L)) and the last two terms denote the coupling between the leads and the two systems as well as the detector–interferometer interaction. According to the Keldysh formulation of electronic transport [12] the coupling to the leads is adiabatically established in order to provide an equilibrium state in the remote past. This is done via the smooth switching function χ_η which obeys the condition $\chi_\eta(-\infty) = 0$, η being the adiabatic parameter. Note that the chemical potentials of the leads are different even in the remote past, but in spite of this finite bias there is no current in the absence of the coupling. The electron–electron interaction is also adiabatically introduced, this simplification meaning that the initial correlations are not taken into account (for more discussions about this problem see the paper by Wagner [13]).

The explicit form of the Hamiltonians is as follows:

$$H_I = \sum_{m\in I} \varepsilon_m d_m^\dagger d_m + \sum_{m\neq n} t_{mn}(\varphi) d_m^\dagger d_n,$$

$$H_D = \varepsilon_0 a^\dagger a, \qquad H_i = U \sum_{m\in Q\,D} d_m^\dagger d_m a^\dagger a,$$

$$H_t = t_{\mathrm{LI}}\left(d_{m_\alpha}^\dagger c_{0\alpha} + d_{m_\beta}^\dagger c_{0\beta}\right) + t_{\mathrm{LD}}\left(a^\dagger c_{0\gamma} + a^\dagger c_{0\delta}\right) + \mathrm{h.c.}$$

d_m, $d_m^\dagger$ are annihilation/creation operators in the mth site of the interferometer and $a^\dagger$, a is the pair of creation/annihilation operators associated with the detector. Similarly we have on leads the pair c, $c^\dagger$. In the case of an Aharonov–Bohm interferometer the hopping coefficients t_{mn} have a Peierls phase due to the magnetic flux φ piercing the ring. H_i describes the Coulomb interaction of strength U between the embedded dot and the detector. H_t couples the interferometer and the detector to the sites 0ν, $\nu = \alpha, \ldots, \delta$ of the lead ν. We denote by m_α the site of the interferometer where the lead α is attached. The corresponding hopping constants are t_{LI} and t_{LD}. The calculation of the current implies computing the statistical average of the corresponding current operator with respect to the time-dependent statistical operator of the coupled system. However, in the long time limit a steady state is achieved in which the non-equilibrium Green's functions depend only on time differences. Using the Langreth rules for the Fourier transforms of the Green–Keldysh function the current through the lead α can be expressed only in terms of the retarded and lesser Green functions at the contact site α (we omit for simplicity the energy dependence of all quantities below; for further details see [11]):

$$\langle J_\alpha\rangle = -\frac{et_{\mathrm{LI}}^2}{\hbar}\int dE\,\rho\,\mathrm{Im}\left(2G_{\alpha\alpha}^R f^\alpha + G_{\alpha\alpha}^<\right). \tag{2}$$

In the above equation ρ is the density of states in the lead and $f_\alpha(E)$ is the Fermi function in the lead α. The main technical problem one faces in computing the current is of course the calculation of interacting Green functions. The Keldysh formalism provides a Dyson equation on the Keldysh–Schwinger contour:

$$G = G_0 + G_0(\Sigma_{\mathrm{L}} + \Sigma_i)G = G_{\mathrm{eff}} + G_{\mathrm{eff}}\Sigma_i G, \tag{3}$$

where G_0 is the contour-ordered Green function of the noninteracting disconnected system and Σ_L and Σ_i are the self-energies due to the leads and to the interaction. The second equation is obtained by summing the perturbation series with respect to the self-energy of the leads and the 'unperturbed' Green function G_{eff} is the noninteracting Green function of the coupled system. When taking explicit components of G on the Keldysh contour the above generalized Dyson equation gives two equations for the retarded and lesser Green function:

$$G^R = G_{\mathrm{eff}}^R + G_{\mathrm{eff}}^R\Sigma_i^R G^R, \tag{4}$$

$$G^< = \left(1 + G^R\Sigma_i^R\right)G_{\mathrm{eff}}^<\left(1 + \Sigma_i^A G^A\right) + G^R\Sigma_i^< G^A, \tag{5}$$

$$G_{\mathrm{eff}}^< = G_{\mathrm{eff}}^R\Sigma_l^< G_{\mathrm{eff}}^A. \tag{6}$$

We shall now derive an equivalent form of Eq. (2) which would help us to understand, at the formal level, the differences between the Landauer formula for noninteracting systems and the current formulas in the interacting case. To be more specific here we shall consider that the interferometer contains a single site dot and we denote this site by d. It is then clear that the interacting self-energy is a matrix which has only one nonvanishing element $\Sigma_{i,dd}$ in the Hilbert space of the interferometer. The self-energy of the leads is instead diagonal in the contact sites and depends only on the retarded Green function of the leads at the endpoints 0ν (see Eq. (16) in [11]). Using the identity $G^R - G^A = 2iG^R\,\mathrm{Im}\,\Sigma^R G^A$, Eq. (5) and the explicit expression for the self-energy of the leads one obtains:

$$\langle J_\alpha\rangle = \frac{et_{\mathrm{LI}}^2}{\hbar}\int_{-2t_L}^{2t_L} dE\left(2\pi\rho^2 G_{\alpha\beta}^R G_{\beta\alpha}^A\left(f^\alpha - f^\beta\right)\right.$$
$$\left. - \rho G_{\alpha d}^R\,\mathrm{Im}\left(2\Sigma_{i,dd}^R f^\alpha + \Sigma_{i,dd}^<\right)G_{d\alpha}^A\right), \tag{7}$$

where the indices of the Green functions represent the contact sites m_α, m_β or the site d in the dot (for example, $G_{\alpha d}^R$ is the Fourier transform of the usual retarded Green function $G_{\alpha d}^R(t,t') = -i\theta(t-t')\langle\{d_{m_\alpha}(t), d^\dagger(t')\}\rangle$. It can be noticed at once that the first term from Eq. (7) resembles the Landauer formula for noninteracting system, but one should keep in mind that the Green functions appearing in this term have to be computed in the presence of electron–electron interaction. The second term in the current formula is a correction to the Landauer formula due to interaction and was not explicitly taken into account in earlier papers. In our previous work [11] we have extensively discussed the nontrivial contribution of this term to the suppression of the quantum coherence. A similar formula holds for the current through the

detector which we shall denote by J_d. As for the interacting self-energies we perform a perturbative calculation with respect to the interaction strength. The formal/technical details are given in [11]. Essentially we compute the first and second order interaction self-energies, which amounts to taking the first diagram in the Hartree class and the polarization bubble. This last diagram contains the inelastic processes in the systems originating from the Coulomb interaction.

3. Results and discussion

We consider now the reduction of the mesoscopic Fano effect in a single-dot Aharonov–Bohm interferometer coupled to a charge detector. The interferometer contains three sites, two of them being (namely, 1 and 3) coupled to the leads. The remaining site (2) is weakly coupled to the other two by a hopping constant which we denote by τ. This site simulates the embedded dot. The detector is also a single level quantum dot coupled to two leads. There is a bias applied on the leads, via the chemical potential in the Fermi functions of each lead. We denote by V_i the bias applied on the interferometer and by V_d the bias applied on the detector. Only the dot-detector Coulomb interaction is considered. This is an approximation and one may argue that for many-level quantum dots the intradot electron–electron interaction could presumably play a role. However, the induced decoherence that we review here is entirely due to the dot-detector interaction.

Fig. 1(a) gives the current through the interferometer as a function of the gate potential V_g applied on the dot. This potential is simulated by adding a constant term to the on-site energy in the Hamiltonian. There are three curves in Fig. 1(a) corresponding to noninteracting case $U = 0$ and to $U = 0.3$ and $U = 0.5$. One can notice at once that the interacting Fano lineshapes are reduced and shifted with respect to the noninteracting Fano line. Also, as the interaction strength increases a bump appears near the Fano dip. Clearly, the visibility of the Fano line is reduced as U increases. It turns out that the second term in the current formula is responsible for the bump in the full current curve given in Fig. 1(a) (for more discussion see [11]). In the presence of Coulomb interaction the charge sensing effect induces a dependence of the current through the detector on the gate potential (we recall that V_g is applied on the embedded dot only). The jump between the two steps increases at larger interaction strength and its location corresponds to the Fano lineshape in Fig. 1(a) (not shown).

We discuss now the suppression of the Aharonov–Bohm oscillations due to the interaction *and* the finite bias on the detector. To this end we fix the gate potential on the dot and vary instead the magnetic flux on the ring. Fig. 1(b) shows curves for the current through the interferometer as a function of the magnetic flux for three values of the interaction strength $U = 0$, $U = 0.3$ and $U = 0.5$. The oscillations are obtained at those values of V_g that correspond to the Fano peaks. The reduction of the AB oscillations is obvious. An important point to be discussed here is the role of the finite bias on the detector. The curves given in Fig. 1 were obtained at $V_d = 1.0$. At lower values of the bias the dephasing decreases at eventually disappears, in good agreement with the experimental data [6]. The theoretical explanation behind this was given in Ref. [11]. Essentially, it can be checked that at finite bias on the detector the imaginary part of the interacting self-energy Σ^R exceeds the self-energy of the leads in the range of energy allowed by the bias window on the interferometer. On the contrary, at small bias $\mathrm{Im}\,\Sigma^R \ll \mathrm{Im}\,\Sigma^{\mathrm{R}}_{\mathrm{L}}$.

As one may expect, the current through the detector depends as well on the magnetic flux, although not in a symmetric fashion. This is shown in Fig. 1(c). However, the oscillations of J_d decrease as U takes larger values. This effect is again a consequence of charge sensing. Also we have investigated the change of the interacting Fano lineshape as function of the magnetic flux. It is well known from the experiments and also from previous theoretical works [14,15] that the sign of the Fano parameter q which gives the asymmetry of the resonance changes as the magnetic flux is varied. We found that this effect is still observable in the interacting case (not shown).

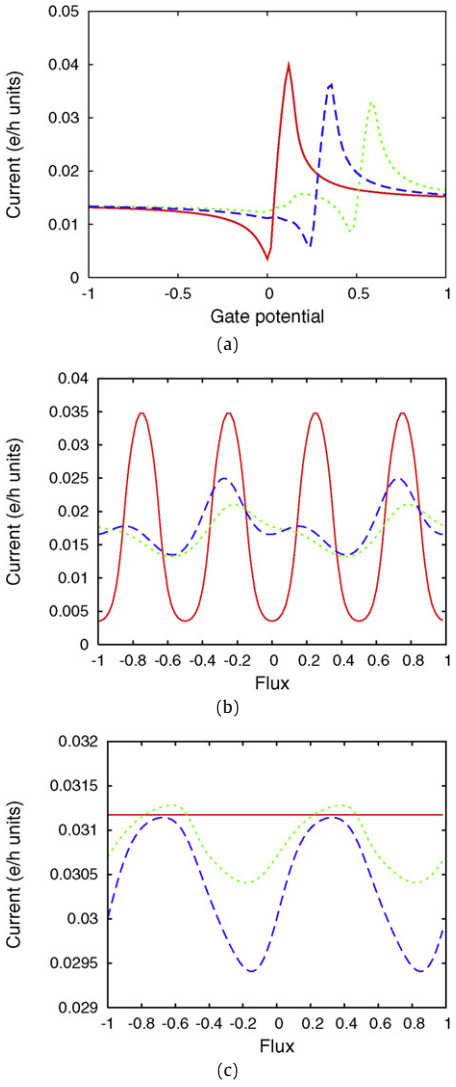

Fig. 1. (Color online.) (a) The total current through the detector as a function of the gate potential applied on the embedded dot, at different interaction strengths. Red line $U = 0$, blue line $U = 0.3$, green line $U = 0.5$. (b) The suppression of the Aharonov–Bohm oscillations due to the charge sensing effect. (c) The charge sensing effect induces a flux dependence of the current through the detector, at fixed gate potential. Other parameters $\tau = 0.2$, $V_d = 1.0$, $V_i = 0.1$.

The previous graphs were obtained with a symmetric bias, that is $\mu_{L,R} = \pm 0.05$ and $\varepsilon_1 = \varepsilon_3 = 0$. Fig. 2(a) shows interacting Fano lines ($U = 0.25$ and $U = 0.5$) for the same bias window which is instead pushed upwards by increasing the chemical potentials of the leads with the same amount. The following facts are noticed: (i) The resonances are shifted to the right, because for higher bias window one needs larger gate potentials to bring the QD level within the transmission region; (ii) The amplitude and the width of the Fano line increase when the bias window moves up. Also the background signal increases (compare also with the background in Fig. 1(a)), suggesting that the distance between the bias window and that part of the interferometer spectrum which gives the background contribution decreases. Evidently, this behavior is not monotonous; for a higher bias window the background signal is

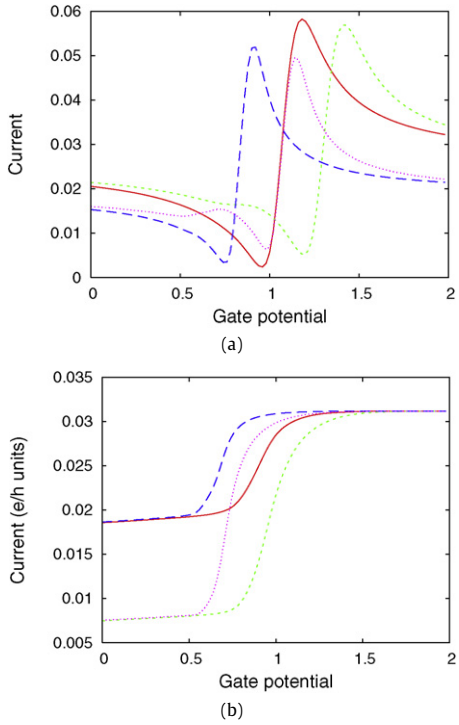

Fig. 2. (Color online.) (a) The Fano lineshapes for two locations of the bias window of the interferometer and for two values of the interaction strength. (b) The current through the detector J_d signals the tunneling into and outside the dot. The red line $U = 0.25$, and the green line $U = 0.5$ correspond to a bias window $[0.65 : 0.75]$. The blue line $U = 0.25$, and the violet line $U = 0.5$ correspond to a bias window $[0.45 : 0.55]$. Other parameters $\tau = 0.2$, $V_d = 1.0$, $V_i = 0.1$.

reduced as the bias window moves away from the spectrum of the truncated ring which is responsible for the background contribution (not shown). (iii) In spite of the changes in the Fano line we just mentioned, Fig. 2(b) shows that the detector exhibits the same jump at resonance, that is, its sensitivity does not depend on the location of the bias window. Note also that the reduction of the Fano line seems to be the same as the one given in Fig. 1(a).

Another result that is meant to complement our analysis of measurement-induced decoherence is presented in Fig. 3. On one hand we plot the amplitude of the Aharonov–Bohm oscillations as a function of the gate potential V_g for both interacting and noninteracting cases. More precisely, for each value of the gate potential we vary the magnetic flux and record the maxima and minima of the Aharonov–Bohm oscillations. This amplitude actually measures the visibility of the AB oscillations. One notices that both curves are not monotonous and have a maximum point. The visibility in the interacting case is lower, as expected. On the other hand we give in the same figure the Fano lines associated with the minima of the AB oscillations (for interacting and noninteracting case). It is easy to see that the maxima of the visibility correspond to the dips of the two Fano lines. Note that even in the interacting case the Fano dip is close to zero, suggesting thus a low dephasing. We have also investigated the two Fano lines at which the AB oscillations reach their maxima. It turns out that the highest visibility is obtained somewhere around the Fano peak (not shown).

4. Conclusions

We have presented the theoretical description of the controlled dephasing in mesoscopic interferometers with quantum dots using

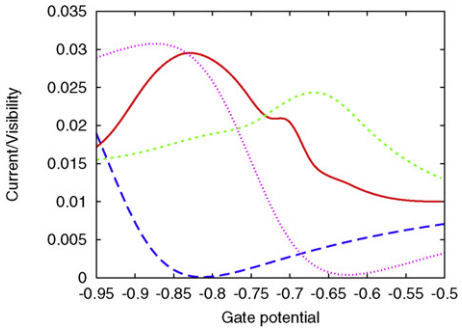

Fig. 3. (Color online.) The visibility (i.e. the amplitude) of the Aharonov–Bohm oscillations as a function of the gate potential: red line $U = 0.0$, green line $U = 0.2$. The two Fano lines are the ones that correspond to the minimum of the AB oscillations: blue line $U = 0.0$, violet line $U = 0.2$. Other parameters: $\tau = 0.2$, $V_d = 1.0$, $V_i = 0.05$.

the non-equilibrium Green–Keldysh formalism for the electronic transport and a perturbative treatment of the electron–electron interaction. The decoherence is induced by the Coulomb repulsion between the charge detector and the embedded dot. Besides the well-known step-like characteristics of the detector current around a Fano resonance we find that the charge sensing effect also induces an oscillatory behavior of this current as a function of the magnetic field. Also, we show that by changing the position of the bias window of the interferometer the Fano line is modified but the detector shows a similar signal. Our formalism can be also used for studying decoherence in interferometers with one of more side-coupled quantum dots [16]. Further investigation of the controlled dephasing should take into account the intradot Coulomb interaction and also more accurate approximations for the Green functions in the presence of electron–electron interaction.

Acknowledgements

B.T. is supported by TUBITAK (No. 106T052) and TUBA. V.M. is supported by TUBITAK-BIDEB and CEEX-2976.

References

[1] A. Yacoby, M. Heiblum, D. Mahalu, H. Shtrikman, Phys. Rev. Lett. 74 (1995) 4047.
[2] R. Schuster, E. Buks, M. Heiblum, D. Mahalu, V. Umanski, H. Shtrikman, Nature 385 (1997) 417.
[3] A.W. Holleitner, C.R. Decker, H. Qin, K. Eberl, R.H. Blick, Phys. Rev. Lett. 87 (2001) 256802.
[4] K. Kobayashi, H. Aikawa, S. Katsumoto, Y. Iye, Phys. Rev. Lett. 88 (2002) 256806; K. Kobayashi, H. Aikawa, S. Katsumoto, Y. Iye, Phys. Rev. B 68 (2003) 235304.
[5] A. Stern, Y. Aharonov, Y. Imry, Phys. Rev. A 41 (1990) 3436.
[6] E. Buks, R. Schuster, M. Heiblum, D. Mahalu, V. Umansky, Nature (London) 391 (1998) 871.
[7] I.L. Aleiner, N.S. Wingreen, Y. Meir, Phys. Rev. Lett. 79 (1997) 3740.
[8] Y. Levinson, Europhys. Lett. 39 (1997) 299.
[9] G. Hackenbroich, Phys. Rep. 343 (2001) 463.
[10] A. Silva, S. Levit, Phys. Rev. B 63 (2001) 201309.
[11] V. Moldoveanu, M. Ţolea, B. Tanatar, Phys. Rev. B 75 (2007) 045309.
[12] C. Caroli, R. Combescot, P. Nozieres, D. Saint-James, J. Phys. C 4 (1971) 916.
[13] M. Wagner, Phys. Rev. B 44 (1991) 6104.
[14] W. Hofstetter, J. König, H. Schoeller, Phys. Rev. Lett. 87 (2001) 156803.
[15] V. Moldoveanu, M. Ţolea, V. Gudmundsson, A. Manolescu, Phys. Rev. B 72 (2005) 085338.
[16] V. Moldoveanu, M. Ţolea, B. Tanatar, Physica E 40 (2008) 1102.